

This is a repository copy of *Testbed Development: An Intelligent O-RAN based Cell-Free MIMO Network*.

White Rose Research Online URL for this paper:

<https://eprints.whiterose.ac.uk/222193/>

Version: Published Version

---

**Article:**

Chu, Yi, Rahmani, Mostafa [orcid.org/0000-0002-7943-9977](https://orcid.org/0000-0002-7943-9977), Shackleton, Josh et al. (4 more authors) (2025) *Testbed Development: An Intelligent O-RAN based Cell-Free MIMO Network*. IEEE Communications Magazine. pp. 74-81. ISSN 0163-6804

<https://doi.org/10.1109/MCOM.001.2400574>

---

**Reuse**

This article is distributed under the terms of the Creative Commons Attribution (CC BY) licence. This licence allows you to distribute, remix, tweak, and build upon the work, even commercially, as long as you credit the authors for the original work. More information and the full terms of the licence here:

<https://creativecommons.org/licenses/>

**Takedown**

If you consider content in White Rose Research Online to be in breach of UK law, please notify us by emailing [eprints@whiterose.ac.uk](mailto:eprints@whiterose.ac.uk) including the URL of the record and the reason for the withdrawal request.

# Testbed Development: An Intelligent O-RAN-Based Cell-Free MIMO Network

Yi Chu, Mostafa Rahmani, Josh Shackleton, David Grace, Kanapathippillai Cumanan, Hamed Ahmadi, and Alister Burr

## ABSTRACT

Cell-free multiple input multiple output (CF-MIMO) systems improve spectral and energy efficiencies using distributed access points (APs) to provide reliable service across an area equivalent to multiple conventional cells. This article presents a novel design and implementation of a CF-MIMO network leveraging the open radio access network (O-RAN) architecture-based testbed to enhance the performance of interference-prone users. The proposed prototype is developed based on open-source software components, and unlike many other prototypes, our testbed is able to serve commercial 5G user equipment (UE). The RAN intelligent controller (RIC) allows the cell-free (CF) network to access the embedded artificial intelligence and benefit from the network optimization techniques that O-RAN brings. The testbed includes an intelligent antenna association xApp, which determines the antenna group that serves each UE based on the live key performance measurements. The article demonstrates the deployment and operation of the CF network and the xApp and discusses how the CF networks can benefit from the O-RAN architecture.

## INTRODUCTION

The rapid evolution of wireless communication technologies necessitates innovative approaches to meet the increasing demands for throughput, coverage, and user experiences. Traditional cellular networks often struggle to provide adequate service for cell-edge users or interference-prone users, primarily due to attenuation and interference from adjacent base stations (BSs). To address these challenges, the concept of cell-free multiple input multiple output (CF-MIMO) networks has emerged as a promising solution [1].

CF-MIMO technology offers a paradigm shift from traditional cellular networks by eliminating cell boundaries and enabling a cooperative network of access points (APs) that jointly serve all user equipment (UE). This approach provides macro-diversity, enhancing coverage and throughput, particularly for interference-prone users. In a CF-MIMO network, a large number of distributed APs, each potentially equipped with multiple antennas, are connected to a central processing unit (CPU) via a fronthaul network, enabling coherent transmission and reception. The CPU operates the system in a distributed MIMO fashion, significantly improving the signal-to-noise

ratio (SNR) and signal-interference-plus-noise ratio (SINR) for users, regardless of their locations. Recent advancements in the implementation of CF-MIMO systems have demonstrated their potential in both centralized and distributed architectures. Centralized architectures, leveraging advanced techniques like minimum mean-square error (MMSE) or zero-forcing (ZF) combining, maximize spectral efficiency and reduce fronthaul signaling compared to standard distributed approaches, while distributed architectures offer flexibility for ultra-dense networks depending on access point cooperation [2].

The evolution toward 6G requires significant improvements in network capacity, spectral efficiency, energy consumption, and reliability [3]. CF-MIMO has been considered a promising architecture for 6G, given its unique benefits to interference-prone users [4]. Open radio access network (O-RAN), as another enabling technology for future mobile networks, provides open interfaces that allow multi-vendor network deployment [5]. O-RAN also disaggregates the RAN into radio units (RU), distributed units (DU), and central units (CU). When multiple RUs are connected to the same DU, the DU naturally becomes the CPU of the CF architecture, which allows the UE to be served by RUs from different vendors simultaneously. The RIC [6] and the customizable RICapps it hosts enable artificial intelligence (AI)-based optimization, including energy efficiency, traffic steering, and dynamic slicing. The network can also benefit from optimization methods unique to the CF architecture, such as serving antenna group association, pilot assignment, UE power control, UE precoding/ combiner techniques, backhaul/fronthaul optimization, and DU/CPU location optimization.

## AVAILABLE CELL-FREE NETWORK TESTBEDS

The mutual benefits and complementary features of the CF and O-RAN architectures have motivated us to develop a prototype to evaluate this hybrid approach. Based on the information available, only the O-RAN compatible fronthaul has been introduced by some of the available CF testbeds. The RIC and E2 interfaces, which are the main enablers of AI, have not yet been implemented. This section reviews key works that have contributed to the development and understanding of CF-MIMO systems.

The work in [7] presents the implementation

*The authors are with University of York, UK.*

Reference	O-RAN Architecture	UE type	Synchronization	MAC Scheduler	Protocol Stack	Modulation/Coding Scheme
[7]	No	SDR	RUs and UEs are synchronized with an Octoclock	Unspecified	OAI 5G PHY stack	Fixed MCS (MCS=10, 16QAM), No MU-MIMO
[8]	No	SDR	RUs are synchronized with PTP	Continuous transmission	Only PHY implemented in Labview	Fixed with QPSK, 16QAM and 64QAM
[9]	No	SDR	RUs are synchronized with PTP	Unspecified	4G stack implemented in Labview	16QAM maximum
[10]	No	similar radio as RU	UEs and RUs are synchronized with PTP and GPS	Unspecified	5G PHY stack	Adaptive MCS with non-standard 48-port DMRS
[11]	Fronthaul only	similar radio as RU	UEs and RUs are synchronized with PTP and GPS	Unspecified	Unspecified	Unspecified
[12]	No	SDR	RUs are synchronized with PTP	Unspecified	5G PHY stack	16QAM maximum
Ours	RIC and E2 included	Commercial 5G UE	RUs are synchronized with an Octoclock	Defined for coexistence of SU and MU-MIMO	Complete 5G stack	Adaptive MCS

TABLE 1. Comparison of CF-MIMO System Implementations.

of CF-MIMO combined with dynamic time division duplex (TDD) using the OpenAirInterface (OAI) 5G stack. Dynamic TDD, which allows cells to schedule uplink (UL) and downlink (DL) slots based on traffic demands, has been integrated with CF-MIMO to mitigate cross-link interference. This testbed has all radios (RU and UE) synchronized to the same reference source and demonstrated the 5G physical layer (PHY) with a fixed modulation and coding scheme (MCS). The authors in [8] demonstrate a distributed CF-MIMO testbed with video streaming. This testbed uses distributed computing without a CPU, thereby reducing fronthaul capacity demands. The testbed consists of 10 APs and 4 UEs (all implemented with software-defined radios (SDRs)), each with a single antenna. The testbed has demonstrated multi-user (MU)-MIMO with UEs served by multiple RUs on the same resource with the Labview 5G PHY stack. The work has been further extended to facilitate the 5G/6G-based private networks suitable for industrial Internet of Things applications [9]. The work proposes a novel orthogonal frequency division multiplexing (OFDM) precoding algorithm, which allows APs in a user-centric cluster to maximize capacity while minimizing interference to neighboring UEs.

The work in [10] proposes a full-spectrum CF-RAN. Key innovations include a scalable CF-MIMO architecture and a CF-MIMO testbed with 64 distributed antennas using commercial radios. The testbed has all radios synchronized with precision time protocol (PTP) and demonstrated 5G MU-MIMO PHY with adaptive MCS and customized 48-port demodulation reference signal (DMRS) signals. The authors in [11] investigate the downlink coherent multi-user transmission in CF-MIMO systems, focusing on over-the-air (OTA) reciprocity calibration and phase synchronization. A testbed including four remote radio units (RRUs) and 4 UEs has been developed to evaluate such an approach. Similar to the work in [10], all radios (RRUs and UEs) are synchronized with PTP. In [12], the authors propose a cloud-based CF-distributed massive MIMO system. The system addresses challenges in synchronization,

calibration, and real-time processing using a 128 128 MIMO setup. The testbed demonstrates 5G PHY with high spectral efficiency and throughput.

### CONTRIBUTIONS

With the review of implemented CF-MIMO prototypes, it is clear that the focus has been on novel low technology readiness level (TRL) PHY technologies. Table 1 offers a concise summary of these works, emphasizing the areas they address and the critical gaps to be investigated. With the latest development of the open-source O-RAN software, we have identified the opportunity to build a mid-TRL testbed with the hybrid CF and O-RAN architecture to demonstrate the benefits of combining the two 6G enabling technologies. Our work aims at developing an intelligent private 5G network to serve commercial-off-the-shelf (COTS) UEs while addressing the gaps identified in Table 1. Our contributions are threefold.

**Full O-RAN Compatible 5G Software Stack:** unlike other CF-MIMO prototypes, which mostly only include PHY, our testbed includes all software components required to serve COTS UEs, such as a full 5G RAN stack, a standalone (SA) 5G core, and a RIC with onboarded xApps. The RAN is designed to be scalable with the number of RUs with the support of MU-MIMO for the UL. To the best of our knowledge, we have not yet noticed any CF-MIMO prototypes that can serve COTS 5G UEs with MU-MIMO. Our testbed is also the first implementation of CF-MIMO on the O-RAN architecture.

**Intelligence Embedded at the RIC:** designed based on the O-RAN architecture, our testbed naturally inherits the AI-driven network optimization from the RIC, which is absent from any existing CF-MIMO prototypes. Many existing O-RAN optimization methods can be directly applied, such as switching RUs on/off for energy saving and proactive UE handover for traffic steering. Novel optimizations for the CF architecture can also be developed, such as UE serving antenna group association (which will be demonstrated later), UE power control, and DU/CPU location optimization.

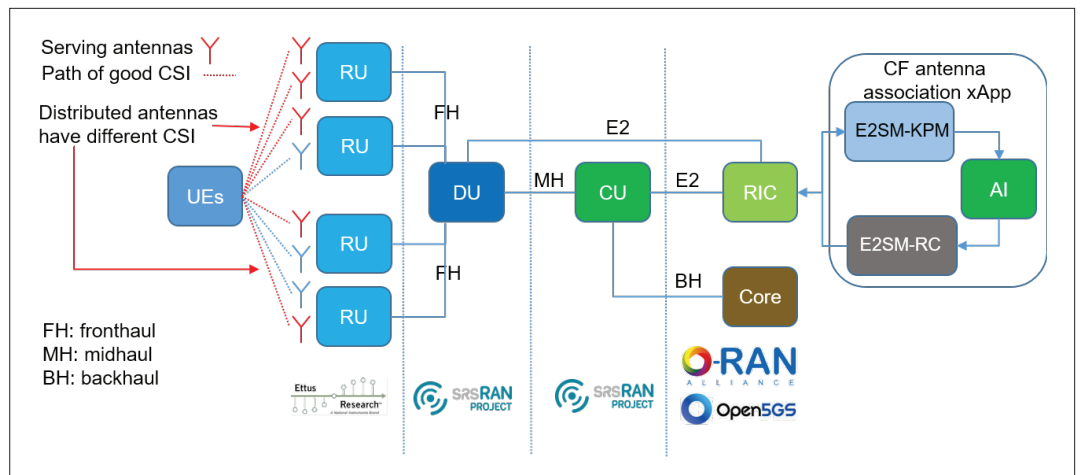


FIGURE 1. O-RAN based cell-free testbed architecture.

### Medium Access Control (MAC) Scheduler:

the MAC scheduler is another critical gap across the existing CF-MIMO prototypes, which is essential for serving COTS UEs. The UEs send scheduling requests (SRs) with different patterns, and the scheduler needs to allocate appropriate resources from the resource grid rather than continuous transmission on the same set of physical resource blocks (PRBs), which is commonly used across existing prototypes. The scheduler of our testbed allows the coexistence of single-user (SU)/MU-MIMO and provides the PHY with the corresponding information for decoding the UE signal.

### SYSTEM MODEL

The testbed is built purely based on open source components (the codebase can be provided upon request). The testbed is designed to validate the CF architecture in an UL scenario which is relatively less restricted (for RAN modifications) compared with DL when serving COTS UEs (which normally do not support more than 4 antennas). Figure 1 shows the architecture of the testbed.

### CU AND DU

These are O-RAN compatible and built based on the srsRAN release 24.04 (<https://github.com/srsran/srsRAN> Project). We have modified the DU significantly to implement MU-MIMO and customized E2 functions to support the CF architecture. Detailed modifications to the MAC scheduler, upper PHY, and the E2 agent will be described later. The modified DU supports a scalable number of antennas for UL and the maximum number of DL antennas remains original (4). The platform for hosting all software components is a Dell PowerEdge R7525 server (64 cores).

### RIC

The testbed includes a dockerized near real-time (Near-RT) RIC from the O-RAN software community (OSC — <https://github.com/srsran/oran-sc-ric>). This is a lightweight version of the original OSC Near-RT RIC Release 1 provided by the srsRAN team. FlexRIC (<https://gitlab.eurecom.fr/mosaic5g/flexric>) also partially operates with the testbed. However, not all RIC report styles are supported by the E2 service model (E2SM)-key performance measurement (KPM), which is a typical interoperability issue across O-RAN vendors.

### INTELLIGENT CF ANTENNA ASSOCIATION xAPP

This xApp is developed within the OSC RIC. The xApp uses E2SM-KPM to collect standardized and customised KPMs and E2SM-RAN control (E2SM-RC) to control the group of antennas which contribute to the UL. We have pretrained a deep Q network (DQN) model which determines the antenna association based on the KPMs. More details of this xApp will be provided in below.

### RU

We use the National Instruments universal software radio peripheral (USRP) X310 as split 8 RUs. Each RU is equipped with 2T2R antennas. All USRPs are synchronized with a common 10 MHz and 1 PPS signal distributed by an Octoclock. This synchronization approach limits the deployment distance between RUs (due to attenuation in coaxial cables), and more practical alternatives are N3xx/N4xx radios, which can be synchronized via the fiber fronthaul using PTP. The testbed includes 4 RUs, which form a 4T8R CF-MIMO network. The number of UL antennas can be further increased if more RUs are available.

### CORE NETWORK

We use Open5GS which is a 5G SA core aligned with 3GPP Release 17.

### UE

Unlike many other CF-MIMO testbeds, our testbed supports COTS 5G handsets. The tested handsets include: Xiaomi 12, Xiaomi 11 Lite 5G NE, Xiaomi Redmi Note 10 5G, Google Pixel 6 and OnePlus Nord 5G. The test SIM cards are from Sysmocom.

### IMPLEMENTATION DETAILS

The original srsRAN DU supports a single RU per DU (cell) with up to 4T4R antennas. We have modified the DU to allow multiple RUs per DU with up to 4TxR antennas (x indicates scalable). With the 4 RUs in our testbed, all RF chains are in use for the first 2 RUs and only RX chains are in use for the other 2 RUs (for UL). 5G includes three physical UL channels: physical random access channel (PRACH), physical uplink control channel (PUCCH), and physical uplink shared channel (PUSCH). Among these, the PRACH



does not support MIMO, the traffic on PUCCH is low, and PUCCH packets are often multiplexed onto PUSCH, so PUSCH becomes our main entry for modifications. The original srsRAN DU supports only SU-MIMO. Upon a UE SR, the MAC scheduler arranges a UL grant and ensures no collisions with previously scheduled UL grants. The UL grant is then packed into a packet data unit (PDU) and sent to the PHY via the functional application platform interface. After receiving the IQ of each slot (14 OFDM symbols), the PHY decodes the PUSCH data of each UE sequentially using the information carried by the corresponding PDU, such as the UE radio network temporary identifier (RNTI), MCS, allocated PRBs, DMRS type, DMRS symbol masks and port, and slot index. All the above procedures need to be modified for MU-MIMO support, and the detailed modifications are described below.

### MAC SCHEDULER FOR MU-MIMO SUPPORT

Figure 2 shows the procedures of the original and modified MAC scheduler. The original scheduler supports only SU-MIMO and ensures no PRB collisions across multiple UEs. The modified scheduler allows a maximum of 2 UEs to share the same PRBs for MU-MIMO. The scheduler allocates PRBs for UEs using round robin on a slot basis, and the modifications prioritize MU-MIMO for better spectral efficiency. At every slot, the modified scheduler checks all UEs for opportunities of MU-MIMO (regardless of new or retransmissions) to maximize the total throughput. The details of the modified scheduler are illustrated below.

The modified MAC scheduler is capable of scheduling multiple UL grants (from multiple UEs) onto the same PRBs while coexisting with SU-MIMO. The original MAC scheduler maintains a bitmap ( $bm\_su$ ) where each bit represents whether each resource element (RE) is occupied by a UE. We have modified  $bm\_su$  so that bit 1 indicates the RE is occupied by at least 1 UE. We have added another bitmap ( $bm\_mu$ ) to represent whether an RE is occupied by only 1 UE. For  $bm\_mu$ , bit 0 indicates that the RE is occupied by 1 UE, and bit 1 indicates that the RE is either not occupied or occupied by 2 UEs. We have also added a vector that stores the UE(s) RNTI(s) allocated to each RE. This vector is used to build the PDU for the PHY.

With every new or pending SR, the scheduler first estimates the required PRBs and MCS based on the UE's channel state information (CSI) and data. The two diamond blocks of low PRB ( $\leq 1$  and  $\leq 2$ ) and MCS ( $< 6$ ) exist because the scheduler has issues scheduling UL grants with only 1 PRB while the MCS is low. The solution of srsRAN is to schedule two PRBs when such a condition is met, and we exclude scheduling such UL grants with MU-MIMO. Otherwise, the scheduler checks  $bm\_mu$  for opportunities for MU-MIMO. If all REs of  $bm\_mu$  are marked as 1 (unsuitable for MU-MIMO), the scheduler checks  $bm\_su$  to find a range of consecutive unoccupied REs that match the request or the longest range of REs possible if there are not enough REs available. Upon successful scheduling, the selected REs in both  $bm\_su$  and  $bm\_mu$  are marked as 1, indicating that these REs can be scheduled to another UE for MU-MIMO.

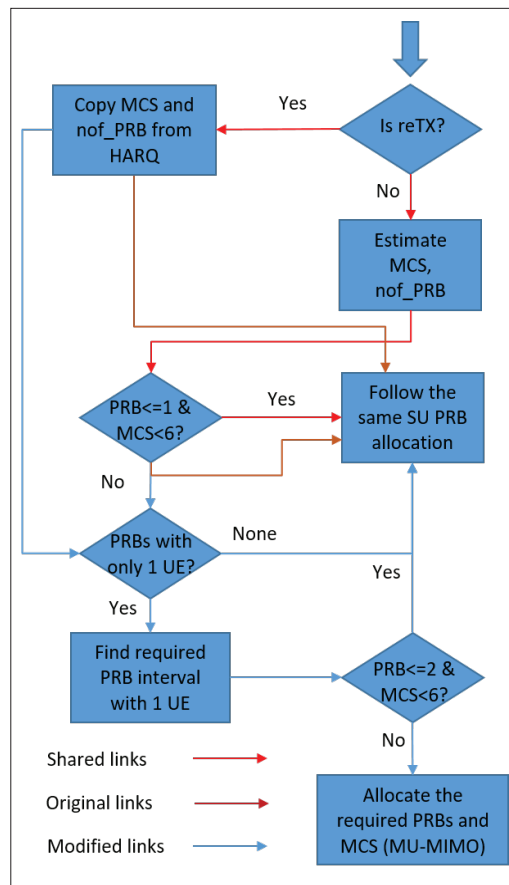


FIGURE 2. Original and modified MAC scheduler logic.

If the scheduler sees opportunities for MU-MIMO, it checks if the conditions in the bottom diamond block are met. If yes, the scheduler skips MU-MIMO scheduling and follows the same steps of using  $bm\_su$  to schedule the UL grant. Otherwise, the scheduler checks  $bm\_mu$  to find a range of consecutive REs available for MU-MIMO that match the request or the longest range of REs possible if there are not enough REs available. Upon successful scheduling, the selected REs in  $bm\_mu$  are marked as 1. These REs should be equal to or a subset of the REs of the first UE allocated to this RE range earlier. The scheduler then finds the REs that Fig. 2: Original and modified MAC scheduler logic are allocated to the first UE and marks them as 1 in  $bm\_mu$ . This avoids the same set of REs being allocated to more than two UEs, which significantly increases the complexity of PHY.

For retransmissions, the scheduler uses the same MCS and number of PRBs of the previous transmission and checks opportunities for MU-MIMO. The rest of the steps are the same as above. After a UL grant is scheduled, the MAC layer builds a PDU that carries the information the PHY needs to decode the PUSCH data. We have modified the PDU format with two additional elements:  $mu\_flag$ , which is a Boolean variable indicating whether this PDU is intended for MU-MIMO, and  $rnti\_mu$ , which stores the RNTI of the other UE when the  $mu\_flag$  is True (the UE scheduled on to unoccupied REs has False  $mu\_flag$ ). The MAC layer also builds a downlink control information (DCI) for the UE, which carries a similar set of information. Within the DCI,

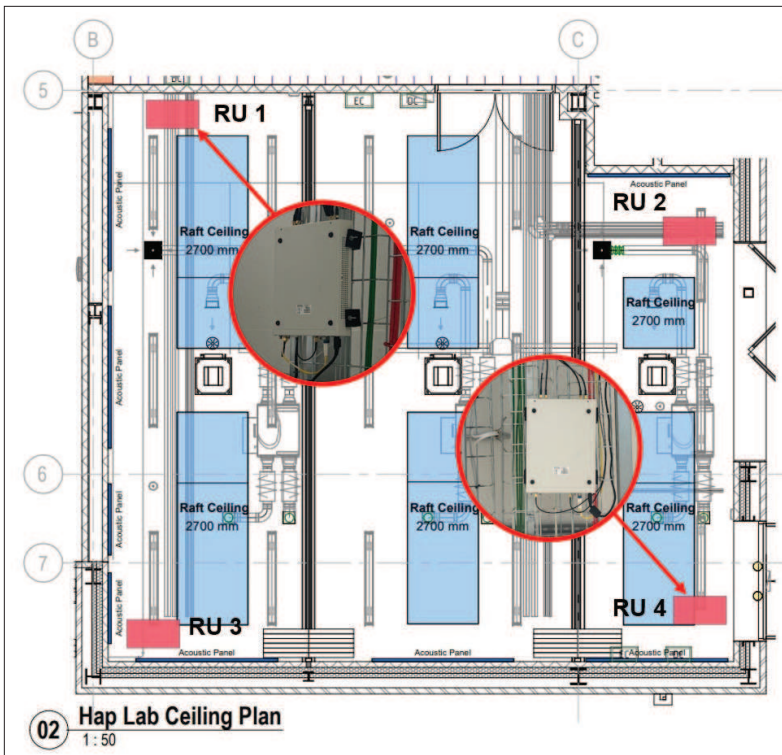


FIGURE 3. Testbed deployment.

the element *antenna\_ports* configure the DMRS ports for the UE according to Table 7.3.1.1.2-8 in [13]. The original MAC layer configures antenna ports=2 (DMRS port 0) for all UEs, and our modification configures different *antenna\_ports* when the *mu\_flag* of the PDU is True. This allows the UEs to use orthogonal DMRS to avoid pilot contamination.

#### UPPER PHY FOR MU-MIMO SUPPORT

At each slot point, the PHY receives a pool of PDUs (from MAC) corresponding to the UEs scheduled within this slot. The original PHY processes the PDUs sequentially, and our modified PHY is capable of processing 2 PDUs (scheduled with MU-MIMO) simultaneously. The PHY first tries to find a PDU with *mu\_flag* set to True. If such a PDU is not found, the PHY processes all PDUs sequentially. If such a PDU exists, the PHY searches the PDU pool again to identify the other PDU that has its UE RNTI matching *rnti\_mu* of the first PDU. These two PDUs are processed together since the channel estimation results of both UEs are needed for the equalizer to separate their IQ. The PHY only processes PDUs with the *mu\_flag* set to False when all PDUs with the *mu\_flag* set to True are processed. We have made significant changes to the PHY's code structure for processing two PDUs in parallel, but most underlying PHY functions remain unchanged such as carrier and sampling frequency synchronization, channel estimation, CSI reporting, demapping, descrambling, and low-density parity-check decoding. The testbed supports UL MU-MIMO only; therefore, reciprocity calibration does not arise. The original PHY utilizes a maximum-ratio combining (MRC) equalizer, which only supports SU-MIMO. We have integrated a ZF equalizer that leverages the CSI from both UEs to equalize two IQ streams [14].

The original srsRAN has a built-in E2 agent that handles the E2 access protocol (E2AP), E2SM-KPM, and E2SM-RC messages between the RAN and the RIC. We have made several modifications to E2SM-KPM and E2SM-RC to implement customized RAN functions for the CF-MIMO architecture. To allow the antenna association xApp to select the most suitable antenna group to serve a UE, we have exposed several non-O-RAN standardized KPMs to the E2 agent. These KPMs are antenna-specific CSI metrics, including the SNR, reference signal received power (RSRP), noise variance, and energy per resource element (EPRE). These can be subscribed by any xApp (that supports the standard E2SM-KPM protocol) using metric names *PUSCH.PORT.SNR*, *PUSCH.PORT.RSRP*, *PUSCH.PORT.NVAR*, and *PUSCH.PORT.EPRE*. We have also exposed the control of the group of antennas that contribute to the equalization of the UE IQ. We have defined a customized RAN parameter ID that any xApp (which supports the standard E2SM-RC protocol) can use to configure on/off of each antenna for a specific UE. The DU maintains the configurations for each UE, and these configurations are used by the MAC layer when building the PHY PDU. We have added a new element, *cf\_port\_selection*, to the UE configurations, which is an array of binary numbers that represent whether each antenna should contribute to equalization. This element is updated every time the E2 agent receives a RAN Control message from the RIC with the corresponding RAN parameter ID included.

#### INTELLIGENT ANTENNA ASSOCIATION xAPP

In this example, xApp can subscribe to 6 O-RAN standardized KPMs and four non-standardized KPMs mentioned earlier. All five RIC report styles are supported, but we prefer style 4, which obtains the KPMs and UE IDs from all UEs. The xApp uses the KPMs as inputs to an embedded DQN, which determines the activation or deactivation of a certain antenna for a UE. This actuation is sent to the RAN via E2SM-RC and ultimately changes the UE configuration *cf\_port\_selection*. The embedded DQN is a lightweight model with three hidden convolutional layers,  $8 \times 4$  input space dimensions, and 16 action space dimensions. The input space consists of the current status of each antenna (aligned with *cf\_port\_selection*), *PUSCH.PORT.SNR*, *PUSCH.PORT.RSRP*, and *PUSCH.PORT.EPRE*. The actions are activating or deactivating a certain antenna. The inference time is generally within the 0.7–2 ms range, and one action per UE is needed for every round of KPMs (every second). Once a set of these KPMs is received for a UE, the DQN generates an action, and the xApp encodes one RAN Control message. The DQN generates actions individually for each UE, and an antenna is only deactivated in the ZF equalizer when both UEs decide to exclude that antenna. Activating more antennas can potentially increase the SNR after equalization but also increase the processing time (roughly 50 ns more per additional antenna per PDU with our testbed) and the reward is computed based on this trade-off. Processing time is critical for a split 8 system (which

has lower and upper PHY on the CPU) and may cause real-time issues if not managed properly. We have implemented a simple simulator to pre-train this DQN since training with a live system would take a significant amount of time.

## TESTBED DEMONSTRATION

This testbed was implemented as part of the YO-RAN (<https://yo-ran.org/>) and REACH (<https://www.reach-oran.org/>) projects. To allow the readers better understanding the features of the testbed, we have prepared a demonstration video (<https://tinyurl.com/52b6pt7y>) with live commentary showcasing the operations. This section describes the configurations of the experiments in detail, explains the showcased functionalities and presents performance measurements.

### EXPERIMENT CONFIGURATIONS

We conducted experiments at the Institute for Safe Autonomy at the University of York. The lab is a 100 m<sup>2</sup> indoor lab and the four RUs are mounted on the roof rails (Fig. 3). The testbed was configured to operate with a 20 MHz bandwidth on the n78 TDD band (the testbed supports up to 100 MHz bandwidth). The maximum DL MCS was configured as 256 QAM, and the maximum UL MCS was configured as 64 QAM (256 QAM was not supported by many COTS UEs). The TDD pattern was configured with six slots assigned for DL and three slots assigned for UL. The two test UEs used in the experiments were a Xiaomi 12 and a OnePlus Nord 5G. The testbed configurations are summarized below in Table 2.

### DEMONSTRATION WALKTHROUGH

The video demonstration starts with the deployment of the components, including the core, the RIC, and the CU/DU. A UE was attached to the network to showcase the throughput performance. The RAN metrics showed that the DL throughput reached a maximum of 127 Mb/s (tested with iperf3) with a 17 MCS (maximum 28) and four layers of data, and the UL throughput reached a maximum of 19 Mb/s with a 28 MCS and one layer of data (COTS UE supports one TX antenna). The combination of higher maximum MCS (256 vs. 64 QAM), a larger number of slots (6 vs. 3), and more layers of data (4 vs. 1) of DL has resulted in a much higher DL throughput compared with UL. This maximum of 19 Mb/s UL throughput was also the maximum cell throughput for the SU-MIMO case since all the PRBs and UL slots were assigned to this UE. A second UE was then attached to the network to showcase the modified MU-MIMO for UL. The UL iperf tests showed that both UEs had a 16 Mb/s throughput, which was not achievable with SU-MIMO of the original srsRAN.

The demonstration then showcased the intelligent antenna association xApp. The xApp subscribed to two O-RAN standardized KPMs (*DRB.UEThpUL* and *DRB.UEThpDL*) and four aforementioned non-standardized KPMs. In the beginning, all antennas had good CSI, and the xApp decided that all antennas should contribute. An anomaly was later manually created to simulate the scenario of the UE being far away from one of the antennas (by disconnecting that antenna). The changes in antenna CSI were observed from the

Configuration Item	Value
Number of DL antennas	4
Number of UL antennas	8
Centre frequency	3600 MHz
Channel bandwidth	20 MHz
Subcarrier spacing	30 kHz
Maximum DL modulation	256 QAM
Maximum UL modulation	64 QAM
TDD pattern periodicity	10 slots
Number of UL/DL slots	3/6 slots
RU output power	15 dBm
E2AP version	R003-v03.00
E2SM-KPM version	R003-v03.00
E2SM-RC version	R003-v03.00

TABLE 2. Testbed Configurations.

Antennas selected	Processor power consumption (W)	Total UE throughput (Mb/s)	PUSCH processing time (us)
8	58.9	38.2	4.1
7	58.2	37.8	3.9
6	57.1	36.2	3.8
5	56.8	35.0	3.7
4	55.8	33.6	3.7
3	55.6	32.3	3.6
2	54.9	29.7	3.6

TABLE 3. Testbed Performance Measurements.

KPMs, and the xApp decided to exclude that antenna from serving the UEs. More anomalies were created to showcase that the pre-trained DQN was reacting to the environmental changes correctly. When the disconnected antennas were reconnected, the xApp decided that these antennas should serve the UEs again.

### PERFORMANCE MEASUREMENTS

Table 3 shows the performance measurements when the xApp selected different numbers of antennas (measurements are averaged across a duration of 30 seconds). The measurements include the energy consumption (logged with Power-TOP) of the processor (which hosts CU/DU/core/RIC), total UE throughput, and the processing time for two MU-MIMO PUSCH PDUs. Two UEs with iperf were used to generate data for MU-MIMO. Similar to the demo video, we have unplugged different numbers of antennas to allow the xApp to deselect them via E2. With each unnecessary antenna removed from the equalizer, the processor energy consumption was reduced by 1 W (or less), and the PUSCH processing time was reduced by 0.2 us (or less). With each useful antenna included in the equalizer, the total throughput gained 0.4 to 2.6 Mb/s. The results show that the xApp can adapt to changing configurations and improve all three measurements.



The original srsRAN uses the least time consuming MRC equaliser. Our ZF equaliser has doubled the processing time per PDU due to various matrix operations (using the Eigen library) and real time issues may appear with larger bandwidth. The equaliser can be further optimized to improve the stability of the RAN.

## CHALLENGES AND FUTURE PATHWAYS

Many challenges remain for implementing the proposed O-RAN based CF network. In this section, we discuss the challenges and future pathways.

### NETWORK SCALABILITY

Multiple challenges exist for large-scale CF network deployment, including UE mobility: although the CF architecture reduces the cell boundaries, in large networks, the mobile UEs will eventually cross the boundaries of multiple DUs due to the physical limitation of the fronthaul distance, and handover is inevitable. Active handover can be implemented to reduce the disruption of UE service. Dense UEs: A CF network should support a scalable number of UEs for MU-MIMO according to the number of distributed antennas available. However, the complexity of MAC and PHY escalates rapidly with the increasing number of UEs, particularly if the scheduler allows the allocation of UEs requesting different numbers of REs into the same RE range. In this case, the PHY needs to process different combinations of UEs sharing various ranges of REs to obtain the transport blocks for a slot, which significantly increases the complexity.

### LIMITED NUMBER OF ORTHOGONAL DMRS

A deterministic aspect for implementing the above bullet point is the number of orthogonal DMRS available. The current srsRAN release supports only type A, which includes eight orthogonal DMRS. When mapping the DMRS ports to antenna ports in the DCI according to Table 7.3.1.1.2-8 in [13], srsRAN only supports a number of DMRS CDM group(s) without data set to 2, which further reduces the number of orthogonal DMRS to four. We have tested all eight type A DMRS with COTS UEs and only antenna ports 2, 4, and 5 have correct channel estimation. In practice, MU-MIMO can support up to three UEs unless the DMRS support is updated.

### PROCESSING TIME FOR MU-MIMO

The original srsRAN uses the least time consuming MRC equaliser. Our ZF equaliser has doubled the processing time per PDU due to various matrix operations (using the Eigen library) and real time issues may appear with larger bandwidth. The equaliser can be further optimized to improve the stability of the RAN.

### MORE RAN CONTROL VIA E2

More configurable parameters can be exposed to support optimizations specific to CF, such as UL UE power control: the PUSCH power is determined by many factors, such as the configurable P0, the number of PRBs, the MCS, and the path loss. An xApp can be designed to allocate the appropriate UL power according to the UE KPMs and MIMO modes. DU/CPU location optimization: it may be beneficial to include as many RUs as possible at a DU/CPU. However, the distance of the fronthaul cannot be extended indefinitely due to the signal latency in fiber. The AI within the RIC can potentially determine the location where the DU/CPU should be deployed, which provides optimal network performance. Interoperability should be considered when expanding RAN Control functions to allow RIC/xApp from multiple vendors to operate

directly. The proposed testbed has exposed customized KPMs and RAN parameters via O-RAN standardized methods, and such principles should persist when implementing new functions.

## CONCLUSIONS

This article presents the design and implementation of an O-RAN-based CF-MIMO network and proposes a novel hybrid network architecture with the use of AI. The presented testbed included a full 5G stack and a video demonstrating the network serving COTS 5G UEs. Key contributions include the implementation of MU-MIMO support, an intelligent antenna association xApp using AI-driven optimizations, and critical modifications to the MAC and PHY layers of the open-source srsRAN. We have also discussed the challenges for improving the capability of the testbed, as well as unique optimization opportunities in the RIC.

### ACKNOWLEDGMENT

This work was supported by project Yorkshire Open Ran (YO-RAN) and project RIC Enabled (CF-)mMIMO For HDD (REACH) funded by the Department for Science, Innovation and Technology (DSIT) of the UK government.

### REFERENCES

- [1] V. Ranjbar et al., "Cell-Free mMIMO Support in the O-RAN Architecture: A PHY Layer Perspective for 5G and Beyond Networks," *IEEE Commun. Standards Mag.*, vol. 6, no. 1, 2022, pp. 28–34.
- [2] E. Björnson and L. Sanguinetti, "Making Cell-Free Massive MIMO Competitive With MMSE Processing and Centralized Implementation," *IEEE Trans. Wireless Commun.*, vol. 19, no. 1, 2019, pp. 77–90.
- [3] W. Jiang et al., "The Road Toward 6G: A Comprehensive Survey," *IEEE Open J. Commun. Society*, vol. 2, 2021, pp. 334–66.
- [4] Y. Zhang et al., "Interdependent Cell-Free and Cellular Networks: Thinking the Role of Cell-Free Architecture for 6G," *IEEE Network*, 2023.
- [5] L. Bonati et al., "Intelligence and Learning in O-RAN for Data-Driven nextG Cellular Networks," *IEEE Commun. Mag.*, vol. 59, no. 10, 2021, pp. 21–27.
- [6] O-RAN, "O-RAN near-RT RIC architecture 4.0," ORAN.WG3.RICARCH-R003-v04.00 Technical Specification, Tech. Rep., 2024; available: <https://orandownload.azurewebsites.net/specifications>.
- [7] H. Kamboj et al., "Hardware Implementation of Cell-Free MIMO and Dynamic TDD Using the OAI 5G NR Codebase," *Proc. 25th Int'l. WSA 2021, ITG Workshop on Smart Antennas*, VDE, 2021, pp. 1–5.
- [8] M. H. Lee et al., "SDR Implementation of a Fully Distributed Cell-Free MIMO System," *Proc. 2022 IEEE Int'l. Conf. Commun. Workshops*, IEEE, 2022, pp. 1–2.
- [9] M. H. Lee et al., "Fully Distributed Cell-Free MIMO Systems: Architecture, Algorithm, and Testbed Experiments," *IEEE Internet of Things J.*, 2023.
- [10] D. Wang et al., "Full-Spectrum Cell-Free RAN for 6G Systems: System Design and Experimental Results," *Science China Information Sciences*, vol. 66, no. 3, 2023, p. 130305.
- [11] Y. Cao et al., "Experimental Performance Evaluation of Cell-free Massive MIMO Systems Using COTS RRU With OTA Reciprocity Calibration and Phase Synchronization," *IEEE J. Sel. Areas Commun.*, vol. 41, no. 6, 2023, pp. 1620–34.
- [12] D. Wang et al., "Implementation of a Cloud-Based Cell-Free Distributed Massive MIMO System," *IEEE Commun. Mag.*, vol. 58, no. 8, 2020, pp. 61–67.
- [13] 3GPP, "S38.212. NR; Multiplexing and Channel Coding, v18.2.0," Technical Specification, 2024.
- [14] M. Rahmani et al., "Deep Reinforcement Learning-Based Sum Rate Fairness Trade-Off for Cell-Free mMIMO," *IEEE Trans. Vehicular Technology*, vol. 72, no. 5, 2022, pp. 6039–55.

### BIOGRAPHIES

Yi CHU received his B.Sc. degree in electronic engineering from China Agriculture University, Beijing, China, in 2008, his M.Sc. degree in communications engineering from the University of York in 2009, and his Ph.D. degree in electronic engineering from the University of York in 2014. He is now a Research



Fellow with the Centre for High Altitude Platform Applications (CHAPA), Institute for Safe Autonomy (ISA), School of Physics, Engineering and Technology, the University of York. His research interests include wireless and quantum communications applications on aerial platforms, AI/ML for O-RAN networks, communications system evaluation using software-defined radio, multi-element antenna array, wireless signal propagation, physical layer network coding, and intelligent medium access control for wireless sensor networks.

MOSTAFA RAHMANI holds a Bachelor of Science degree in Electrical Engineering from Shiraz University, obtained in 2009. He furthered his education with a Master of Science in Communication Systems Engineering from Tarbiat Modares University in Tehran, completing this in 2012. In 2023, he earned his Ph.D. in Communication Systems Engineering from Shiraz University of Technology. Currently serving as a postdoctoral researcher at the University of York, Mostafa specializes in advanced wireless communication systems. His research ambitiously integrates machine learning and deep reinforcement learning into next-generation wireless technologies. His areas of expertise include MIMO, cell-free massive MIMO, Open RAN, and physical layer network coding, with a keen focus on pioneering artificial intelligence applications within these domains.

JOSH SHACKLETON is currently a technical specialist at the Centre for High Altitude Platform Applications (CHAPA), School of Physics, Engineering and Technology, University of York. A multidisciplinary engineer with experience in research fields including High Altitude Platforms, communication systems, vacuum/space technologies, and beam profile gas detectors.

DAVID GRACE [S'95, A'99, M'00, SM'13] received his PhD from the University of York in 1999. He is now Professor (Research) and leads the Challenging Environments Research Theme in the School of Physics, Engineering, and Technology, and is pillar lead for Advanced Communications in the university's Institute for Safe Autonomy and Director of the Centre for High Altitude Platform Applications. Current research interests include aerial platform-based communications, the application of artificial intelligence to wireless communications, 5G system architectures, dynamic spectrum access, and interference management. He is recently a lead investigator on UK government-funded MANY, dealing with 5G trials in rural areas, and currently leads HiQ investigating Quantum Key Distribution from high altitude platforms. He is also leading the UK government-funded YO-RAN and REACH projects which develop O-RAN testbeds and trials. He was the technical lead on the 14-partner FP6 CAPANINA project that dealt with broadband communications from high-altitude platforms. He is the author of over 280 papers and the author/editor of 2 books.

KANAPATHIPPILLAI CUMANAN [SM] received a B.Sc. degree (with First-Class Hons.) in electrical and electronic engineering from the University of Peradeniya, Sri Lanka, in 2006 and a Ph.D. degree in signal processing for wireless communications from Loughborough University, Loughborough, UK, in 2009. He is currently a Senior Lecturer with the School of Physics, Engineering and Technology, University of York, U.K. From March 2012 to November 2014, he worked as a Research Associate with the School of Electrical and Electronic Engineering, Newcastle University, UK. Prior to this, he was with the School of Electronic, Electrical and System Engineering, Loughborough University. In 2011, he was an academic visitor to the Department of Electrical and Computer Engineering, National University

of Singapore, Singapore. From January 2006 to August 2006, he was a Teaching Assistant with the Department of Electrical and Electronic Engineering, University of Peradeniya. He was a research student at Cardiff University, Wales, U.K., from September 2006 to July 2007. He has published more than 100 journal articles and conference papers, which attracted more than 4000 Google Scholar citations. His research interests include nonorthogonal multiple access, cell-free massive MIMO, physical layer security, cognitive radio networks, convex optimization techniques, and resource allocation techniques. He was the recipient of an Overseas Research Student Award Scheme from Cardiff University. He is currently serving as an Associate Editor for IEEE Wireless Communications Letters and IEEE Open Journal of Communications Society.

HAMED AHMADI is a Reader in Digital Engineering at the School of Physics, Engineering and Technology, University of York, UK. He is also an adjunct academic at the School of Electrical and Electronic Engineering, University College Dublin, Ireland. He received his Ph.D. from the National University of Singapore in 2012, where he was a SINGA PhD scholar at the Institute for Infocomm Research, A-STAR. Since then he worked at different academic and industrial positions in the Republic of Ireland and the UK. He has published more than 100 peer-reviewed book chapters, journal and conference papers. He is an associate editor and chief of IEEE Communication Standards magazine and a fellow of the UK Higher Education Academy. He has been the network working group chair of COST Actions CA15104 (IRACON) and CA20120 (INTERACT). He had to chair roles in organizing and technical program committees of several IEEE flagship conferences, including IEEE ICC 2024, EUCNC 2019, PIMRC 2024, and 2019. He is also the treasurer of the IEEE UK and Ireland Diversity, Equity, and Inclusion Committee. His current research interests include the design, analysis, and optimization of wireless communications networks, the application of machine learning in wireless networks, Open Radio Access and Networking, green networks, airborne networks, Digital twins of networks, and Internet-of-Things.

ALISTER G. BURR [SM] was born in London, U.K., in 1957. He received a B.Sc. degree in electronic engineering from the University of Southampton, Southampton, UK, in 1979 and a Ph.D. degree from the University of Bristol, Bristol, U.K., in 1984. Between 1975 and 1985, he was with Thorn-EMI Central Research Laboratories, London. In 1985, he joined the Department of Electronics (now Electronic Engineering) at the University of York, York, UK, where he has been a Professor of Communications since 2000. His research interests include wireless communication systems, especially MIMO, cooperative systems, physical layer network coding, and iterative detection and decoding techniques. He has authored or coauthored around 250 papers in refereed international conferences and journals and is the author of *Modulation and Coding for Wireless Communications* (published by Prentice-Hall/PHEI), and coauthor of *Wireless Physical-Layer Network Coding* (Cambridge University Press, 2018). In 1999, he was the recipient of the Senior Research Fellowship by the U.K. Royal Society, and in 2002, he received the J. Langham Thompson Premium from the Institution of Electrical Engineers. He has also given more than 15 invited presentations, including three keynote presentations. He was the Chair, working group two, of a series of European COST Programmes, including IC1004 Cooperative Radio Communications for Green Smart Environments, and was also an Associate Editor for IEEE Communications Letters, Workshops Chair for IEEE ICC 2016, and the TPC Co-Chair for PIMRC 2018 and 2020.